β-Hydroxybutyrate inhibits histone deacetylase 3 to promote claudin-5 generation and attenuate cardiac microvascular hyperpermeability in diabetes

Bin Li[1] · Yijin Yu[2] · Kun Liu[1] · Yuping Zhang[2] · Qi Geng[2] · Feng Zhang[1] · Yanning Li[1,2] · Jinsheng Qi[1]

Abstract

Aims/hypothesis Microvascular endothelial hyperpermeability, mainly caused by claudin-5 deficiency, is the initial pathological change that occurs in diabetes-associated cardiovascular disease. The ketone body β-hydroxybutyrate (BHB) exerts unique beneficial effects on the cardiovascular system, but the involvement of BHB in promoting the generation of claudin-5 to attenuate cardiac microvascular hyperpermeability in diabetes is poorly understood.

Methods The effects of BHB on cardiac microvascular endothelial hyperpermeability and claudin-5 generation were evaluated in rats with streptozotocin-induced diabetes and in high glucose (HG)-stimulated human cardiac microvascular endothelial cells (HCMECs). To explore the underlying mechanisms, we also measured β-catenin nuclear translocation, binding of β-catenin, histone deacetylase (HDAC)1, HDAC3 and p300 to the *Claudin-5* (also known as *CLDN5*) promoter, interaction between HDAC3 and β-catenin, and histone acetylation in the *Claudin-5* promoter.

Results We found that 10 weeks of BHB treatment promoted claudin-5 generation and antagonised cardiac microvascular endothelial hyperpermeability in rat models of diabetes. Meanwhile, BHB promoted claudin-5 generation and inhibited paracellular permeability in HG-stimulated HCMECs. Specifically, BHB (2 mmol/l) inhibited HG-induced HDAC3 from binding to the *Claudin-5* promoter, although nuclear translocation or promoter binding of β-catenin did not change with BHB treatment. In addition, BHB prevented the binding and co-localisation of HDAC3 to β-catenin in HG-stimulated HCMECs. Furthermore, using mass spectrometry, acetylated H3K14 (H3K14ac) in the *Claudin-5* promoter following BHB treatment was identified, regardless of whether cells were stimulated by HG or not. Although reduced levels of acetylated H3K9 in the *Claudin-5* promoter were found following HG stimulation, increased H3K14ac was specifically associated with BHB treatment.

Conclusions/interpretation BHB inhibited HDAC3 and caused acetylation of H3K14 in the *Claudin-5* promoter, thereby promoting claudin-5 generation and antagonising diabetes-associated cardiac microvascular hyperpermeability.

Keywords Claudin-5 · Diabetes-associated cardiovascular disease · HDAC3 · H3K14ac · β-Hydroxybutyrate · Microvascular hyperpermeability

---

Bin Li, Yijin Yu and Kun Liu contributed equally to this work.

✉ Yanning Li
liyanning1981@126.com

✉ Jinsheng Qi
qijinsheng777@163.com

[1] Department of Biochemistry, College of Integrated Chinese and Western Medicine, Hebei Medical University, Hebei, People's Republic of China

[2] Department of Molecular Biology, Hebei Key Lab of Laboratory Animal Science, Hebei Medical University, Hebei, People's Republic of China

Research in context

What is already known about this subject?

- Claudin-5 insufficiency is a major contributor to microvascular endothelial hyperpermeability in diabetes

- β-Hydroxybutyrate (BHB) exhibits unique cardiovascular protective effects

- BHB inhibits type 1 histone deacetylases (HDACs) to elevate histone acetylation and activate the expression of protective genes

What is the key question?

- How is BHB involved in the claudin-5-mediated attenuation of diabetes-associated cardiac microvascular hyperpermeability?

What are the new findings?

- BHB promoted claudin-5 generation and antagonised cardiac microvascular endothelial hyperpermeability in vivo and in vitro

- BHB inhibited high-glucose-induced HDAC3 from binding to the *Claudin-5* (also known as *CLDN5*) promoter and β-catenin

- BHB caused specific acetylation of H3K14 in the *Claudin-5* promoter

How might this impact on clinical practice in the foreseeable future?

These findings may contribute to a better understanding of the cardiovascular protective effects of BHB and provide important evidence for its clinical applications for claudin-5 deficiency-driven endothelial hyperpermeability

Abbreviations

BHB	β-Hydroxybutyrate
BHB1	Diabetes mellitus+low concentration BHB group
BHB2	Diabetes mellitus+intermediate concentration BHB group
BHB3	Diabetes mellitus+high concentration BHB group
ChIP	Chromatin immunoprecipitation
Co-IP	Co-immunoprecipitation
DM	Diabetes mellitus (group)
HCMEC	Human cardiac microvascular endothelial cell
HDAC	Histone deacetylase
HG	High glucose
L-HG	High L-glucose
H3K9ac	Acetylated H3K9
H3K14ac	Acetylated H3K14
LG	Low glucose
STZ	Streptozotocin
TRITC	Tetramethylrhodamine

Introduction

Cardiovascular disease is the principal cause of death and morbidity among people with diabetes, who have a two- to fourfold increased cardiovascular risk compared with adults without diabetes [1]. The cardiac microvasculature refers to vessels <150 μm in diameter, which provide nutrients and remove metabolic byproducts within the heart tissue [2]. Endothelial dysfunction is the initial factor and early pathological manifestation leading to diabetic microvascular diseases, which are believed to play important pathophysiological roles in the development of heart failure [3, 4].

Endothelial tight junctions control paracellular permeability, serving as an important barrier to maintain vascular homeostasis in blood vessels [5]. Disruption of tight junctions is a hallmark event in endothelial barrier dysfunction, leading to paracellular hyperpermeability in diabetes [6]. Cardiac microvascular hyperpermeability leads to leakage of pathological factors that trigger subsequent fibrosis or cardiomyocyte damage [6, 7]. However, the underlying mechanism of cardiac microvascular hyperpermeability in diabetes has not been clarified and there is no effective therapy.

Claudin-5 is considered the main component of endothelial tight junctions, where it plays a crucial role in the control of endothelial permeability [8]. In diabetes, claudin-5 dysfunction is a major contributor to microvascular hyperpermeability [9]. Our previous study showed that claudin-5 expression was suppressed in high glucose (HG)-stimulated human cardiac microvascular endothelial cells (HCMECs) [10]. The Wnt/β-catenin signalling pathway is essential for the maintenance of endothelial homeostasis [11]. Following the binding of Wnt ligand to its receptor, β-catenin is translocated to the nucleus to regulate the transcription of target genes, including

Claudin-5 (also known as *CLDN5*) [12]. Additionally, histone modification, particularly acetylation of lysine residues, acts as an on/off switch for gene transactivation [13, 14]. Acetyltransferase and histone deacetylases (HDACs) are 'writers' and 'erasers' of histone acetylation, respectively, tightly controlling gene transcription. As a key transcriptional co-activator, acetyltransferase p300 is involved in the transactivation of pathological genes in cardiovascular diseases [13]. Relating to acetyltransferase, members of the HDAC family have different roles, and type 1 HDACs, particularly HDAC3, are believed to be the main contributors to cardiovascular disease in diabetes [14, 15]. However, it is unclear whether changes in β-catenin or its recruitment with the co-factors HDACs or p300, lead to suppressed claudin-5 transcription and cardiac microvascular hyperpermeability in diabetes.

In situations of insufficient glucose supply, such as starvation, ketone bodies are generated to provide energy [16]. Although a sharp increase in ketone bodies can cause ketoacidosis in individuals with diabetes, moderate increases (<10 mmol/l) have been reported to have important protective roles [17]. The main component of ketone bodies, β-hydroxybutyrate (BHB), has been recently characterised as a biologically active molecule with multiple beneficial roles [18]. Besides supplying energy, BHB has various cardiovascular protective effects that are especially strong in endothelial cells [19–21]. We have published a series of studies in rat models of diabetes, demonstrating that BHB treatment elevated the expression of vascular endothelial growth factor to alleviate aortic endothelial injury, and promoted the generation of matrix metalloproteinase-2 to antagonise glomerulosclerosis [22, 23]. A broad spectrum of targets has been proposed for the protective effects of BHB [18]. BHB has been reported to bind to a membrane receptor, interact with key functional proteins or inhibit the nucleotide-binding domain leucine-rich repeat (NLR) and pyrin domain containing receptor 3 (NLRP3) inflammasome [20, 24, 25]. Notably, BHB enters the nucleus and inhibits type 1 HDACs to elevate histone acetylation and activate the expression of protective genes [26]. Although BHB exhibits conspicuous cardiovascular protective effects, there is no report of the effects of BHB on β-catenin, and no one has investigated whether it inhibits HDACs to activate *Claudin-5* transcription and antagonise cardiac microvascular hyperpermeability in diabetes.

In this study, we aimed to evaluate BHB-induced claudin-5 generation and antagonism of cardiac microvascular hyperpermeability in rat models of diabetes. We also aimed to verify the effects of BHB on claudin-5 generation and paracellular hyperpermeability in HG-stimulated HCMECs. The mechanism by which BHB promotes claudin-5 generation was explored through measurements of β-catenin nuclear translocation, binding of β-catenin, HDAC1, HDAC3 and p300 to the *Claudin-5* promoter, interaction between β-catenin and HDAC3, and histone acetylation in the *Claudin-5* promoter in HG-stimulated HCMECs.

Methods

Animal experiments Animal care and use were performed in accordance with the procedures outlined in the National Institutes of Health Guidelines and the experimental protocol was approved by the Institutional Ethics Committee of Hebei Medical University (Hebei, People's Republic of China). Seventy healthy male Sprague Dawley rats (210.38 ± 26.25 g; 6 weeks old) and their standard chow were provided by the Department of Experimental Animals of Hebei Medical University. Rats were maintained in a controlled environment (12 h dark–light cycles; 22–24°C; humidity 50–60%) with free access to water and chow. Rats were randomly divided into five groups: diabetes mellitus ('DM'; $n = 15$); DM+low concentration BHB ('BHB1'; $n = 15$); DM+intermediate concentration BHB ('BHB2'; $n = 15$); DM+high concentration BHB ('BHB3'; $n = 15$); and control ('Con'; $n = 10$). The former four DM groups were injected intraperitoneally with streptozotocin (STZ; 40 mg/kg, dissolved in freshly made 0.1 mol/l citrate buffer, pH 4.4, 10 mg/ml) to induce diabetes, as previously reported [27]. Rats in the BHB1, BHB2 and BHB3 groups were injected subcutaneously with $160 \ \mathrm{mg \ kg^{-1} \ day^{-1}}$, $200 \ \mathrm{mg \ kg^{-1} \ day^{-1}}$ and $240 \ \mathrm{mg \ kg^{-1} \ day^{-1}}$ BHB (Sigma, Steinheim, Germany), respectively [22, 23]; rats in the DM and Con groups were administered an equivalent volume of saline (154 mmol/l NaCl). Fasting blood glucose and body weight were measured at 3 days and 10 weeks after diabetes induction. At the end of the experiment, FITC-labelled dextran was used to measure cardiac and mesenteric microvascular endothelial permeability in vivo. After the rats were killed, a segment of heart tissue was collected for H&E staining and claudin-5 immunofluorescence staining, and another segment was used for the detection of claudin-5 mRNA expression and protein content.

Microvascular permeability FITC-dextran (70 kDa; Sigma-Aldrich, Munich, Germany) was used in the measurement of cardiac microvascular permeability in vivo [28]. Rats were anaesthetised and treated with FITC-dextran (20 mg in 1 ml saline) through caudal vein injection. Thirty min after injection, the animals were killed and heart tissue was taken out and frozen immediately. After being cut, frozen sections were observed and imaged using a fluorescence microscope (IX51; Olympus, Tokyo, Japan). In addition, when the rats were killed, mesentery was taken out immediately for the observation of mesenteric microvessels using a fluorescence microscope.

Cells and treatments HCMECs without mycoplasma contamination were purchased from ScienCell and cultured in Endothelial Cell Medium (ScienCell, Carlsbad, USA) with 5 mmol/l glucose and 10% (vol./vol.) fetal bovine serum. After the cells were treated with 20 mmol/l, 25 mmol/l, 30 mmol/l and 35 mmol/l HG for 24 h, *Claudin-5* mRNA expression and paracellular permeability were measured to verify the optimal HG concentration for claudin-5 suppression and paracellular hyperpermeability. Subsequently, the cells were divided into low glucose (LG, 5 mmol/l), high L-glucose (L-HG; 25 mmol/l), HG (25 mmol/l) and HG+BHB (1 mmol/l, 2 mmol/l, 4 mmol/l) groups. mRNA expression and protein content of claudin-5, as well as paracellular permeability, were measured following 24 h treatment. In addition, the cellular distribution of claudin-5 was detected following 2 mmol/l BHB treatment. Furthermore, the content and nuclear translocation of β-catenin, and the binding of β-catenin, HDAC1, HDAC3 and p300 to the *Claudin-5* promoter were measured. The binding and co-localisation of HDAC3 and β-catenin were detected; therefore, associated histone acetylations in the *Claudin-5* promoter were analysed.

Paracellular permeability assay HCMECs were cultured on transwell inserts (Fisher Scientific, Corning, NY, USA) until confluent. Then 70 kDa FITC-dextran (1 mg/ml final concentration) was added to the culture medium in the upper chamber. After 1 h incubation, the concentration of FITC-dextran transferred to the lower chamber was determined using a microplate reader (SpectraMax i3; Molecular Devices, San Jose, CA, USA) with excitation and emission wavelengths of 490 nm and 530 nm, respectively.

Quantitative RT-PCR mRNA expression of *Claudin-5* was quantified by quantitative RT-PCR. Total RNA was isolated using Trizol reagent (Takara, Dalian, China) and reverse transcribed into cDNA using the RevertAid First Strand cDNA Synthesis Kit (Fermentas, Shanghai, China), followed by quantitative real-time PCR amplification using specific primers (see electronic supplementary material [ESM] Table 1). 18S RNA primers were used as an internal standard.

Immunofluorescence Cellular distribution of claudin-5 and nuclear translocation of β-catenin were detected by immunofluorescence, as previously reported [10]. The primary antibodies used were anti-claudin-5 (1:50 dilution in PBS; catalogue no. BS1069; Bioworlde, Nanjing, China), anti-CD31 (1:50 dilution in PBS; catalogue no. GB12063; Servicebio, Wuhan, China) or anti-β-catenin (1:50 dilution in PBS; catalogue no. sc-7963; Santa Cruz, Starr County, TX, USA), and the corresponding secondary antibodies were FITC- or tetramethylrhodamine (TRITC)-conjugated (1:20 dilution in PBS; catalogue no. ZF0312 or ZF0316; Zhongshan, Beijing, China), with DAPI being used for nucleus staining. Images

were observed under a fluorescence microscope (IX51; Olympus). To get exact results, controls (PBS instead of the primary or secondary antibody) were designed to eliminate background noise.

DNA pull-down Contents of β-catenin, HDAC1, HDAC3, p300, acetylated H3K9 (H3K9ac) and acetylated H3K14 (H3K14ac) bound to the *Claudin-5* promoter were measured by DNA pull-down assay. Cells were collected and nuclear proteins were fractionated using a nuclear extraction kit (BestBio, Shanghai, China). After protein concentration was determined, we performed a DNA affinity precipitation assay. Oligonucleotides that contained biotin on the 5′ end of each strand were used. Sequences of oligonucleotides for the β-catenin binding site and the mutant binding site are presented in ESM Table 2. Each pair of oligonucleotides was annealed according to standard protocols. Nuclear protein extracts (200 μg) were precleared with ImmunoPure streptavidin-agarose beads (20 μl/sample; Thermo Fisher Scientific, Waltham, MA, USA). After centrifugation, the supernatant was incubated with 4 μg of biotinylated double-stranded oligonucleotides overnight. Streptavidin-agarose beads (20 μl) were added and incubated for 4 h, and the protein–DNA–streptavidin–agarose complex was subjected to western blotting or mass spectrometry. Mass spectrometry was performed by Jingjie PTM Biolab (Hangzhou, China).

Chromatin immunoprecipitation The binding of β-catenin to the *Claudin-5* promoter was analysed by chromatin immunoprecipitation (ChIP), performed as previously described [27]. In brief, anti-β-catenin antibody (4 μg) or control rabbit IgG (both Santa Cruz) were added to the sonicated lysate, and then protein G agarose beads (20 μl/sample; Santa Cruz) were used for immunoprecipitation. Primers for the predicted β-catenin binding site in the human *Claudin-5* promoter (Gene ID: 7122) were as follows: β-catenin–*Claudin-5* (forward) 5′-GCCCTGTCCAATGGAAC-3′, β-catenin–*Claudin-5* (reverse) 5′-CATTTCTCGAAAGGTCCAC-3′; with a 235 bp product.

Co-immunoprecipitation Binding of HDAC1, HDAC3 and p300 to β-catenin was analysed by co-immunoprecipitation (Co-IP) assay using previously described methods [27]. In brief, nuclear extracts were re-suspended in ice-cold immunoprecipitation buffer, reacted with anti-β-catenin antibody (2 μg; Santa Cruz) and incubated with protein G agarose (20 μl/sample; Santa Cruz) overnight. Co-immunoprecipitated HDAC1, HDAC3 and p300 was detected by western blotting. Conversely, anti-HDAC3 antibody (2 μg; catalogue no. ab137704; Abcam, Shanghai, China) was used and co-immunoprecipitated β-catenin was detected by western blotting. Nuclear

β-catenin, HDAC1, HDAC3 or p300 was used as the input and β-actin as a loading control.

Western blotting Protein levels of claudin-5, β-catenin, HDAC1, HDAC3, p300, H3K9ac and H3K14ac were detected by western blotting, using a previously described protocol [10, 27]. The antibodies used were: anti-claudin-5 (1:200 dilution in PBS; Bioworlde), anti-β-catenin (1:200 dilution in PBS; Santa Cruz), anti-HDAC1 (1:1000 dilution in PBS; catalogue no. ab7028; Abcam), anti-HDAC3 (1:1000 dilution in PBS; Abcam), anti-p300 (1:500 dilution in PBS; catalogue no. NB500–161; Novus Biologicals, Littleton, CO, USA), anti-H3K9ac (1:500 dilution in PBS; catalogue no. 9649S; CST, Shanghai, China), anti-H3K14ac (1:500 dilution in PBS; catalogue no. 7627S; CST), anti-H3 (1:1000 dilution in PBS; catalogue no. 4499S; CST) and anti-β-actin (1:2000 dilution in PBS; catalogue no. D110001; Sangon Biotech, Shanghai, China). Band intensity was quantified by Quantity One v4.6.2 software (Bio-Rad, Shanghai, China) and calculated as indicated.

Confocal microscopy Co-localisation of HDAC3 and β-catenin was measured by confocal detection, as previously described [27]. The primary antibodies used were anti-HDAC3 (1:50 dilution; Abcam) and anti-β-catenin (1:50 dilution in PBS; Santa Cruz), and the secondary antibodies used were FITC- and TRITC-conjugated (1:20 dilution in PBS; catalogue no. ZF0311 and ZF0313; Zhongshan). Images were obtained during the same intervals between samples with a laser confocal scanning microscope (Olympus). To get exact results, controls (PBS instead of the first antibody or the second antibody) were designed to eliminate background noise.

Statistical analysis Data are presented as means±SD from distinct samples. One-way ANOVA was used to analyse differences among groups, and differences between two groups were evaluated using the least significant difference test (two-tailed). Values of $p < 0.05$ were considered statistically significant. Experiments were not randomised or blinded. Rats of accidental death or outrageous deviation were
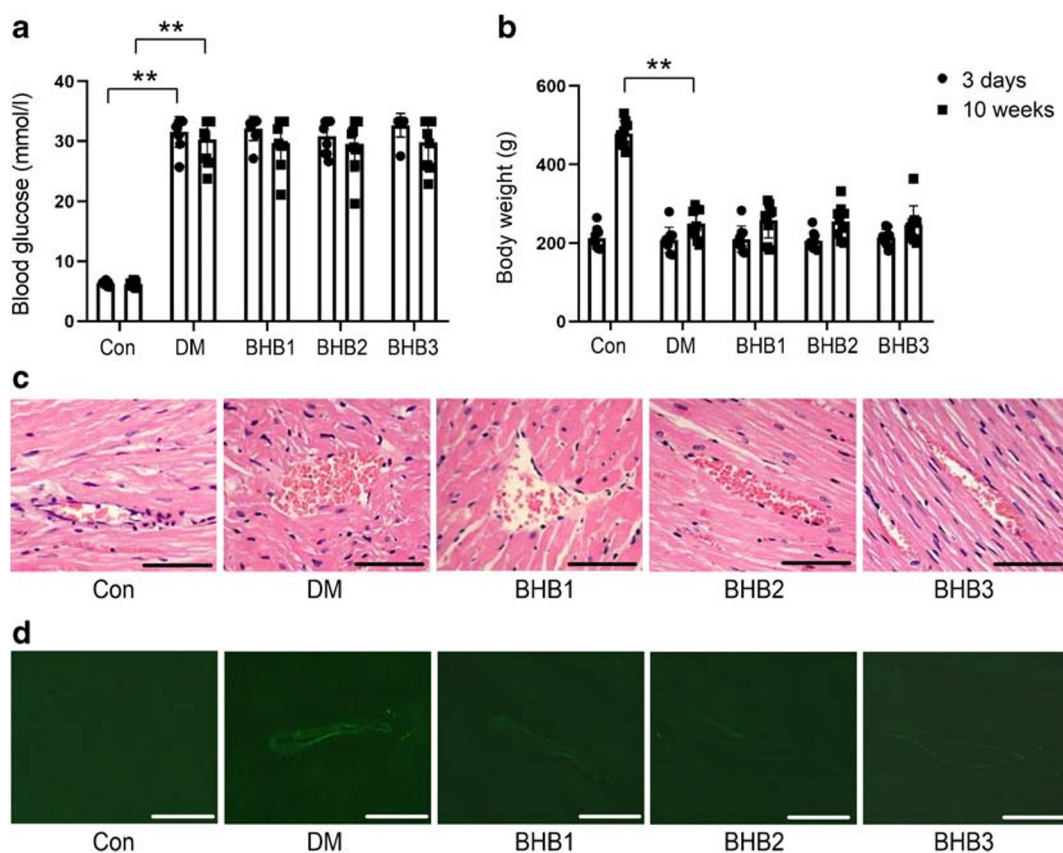

Fig. 1 BHB attenuated cardiac microvascular hyperpermeability in the diabetic rats. Changes in blood glucose (**a**) and body weight (**b**) in rats treated for 3 days or 10 weeks with STZ alone (DM), or STZ plus 160 mg kg^{-1} day^{-1} BHB (BHB1), 200 mg kg^{-1} day^{-1} BHB (BHB2) or 240 mg kg^{-1} day^{-1} BHB (BHB3) ($n = 9$). Data are means±SD. (**c**) H&E staining showed cardiac microvascular endothelial injury. (**d**) To assess cardiac microvascular permeability after 10 weeks of BHB treatment, the fluorescence of heart sections following injection of rats with FITC-dextran for 30 min was analysed. Scale bars, 50 μm. Images are representative of ten visual fields per group. **$p < 0.01$ vs DM, one-way ANOVA and least significant difference test

excluded for the data statistics of blood glucose and body weight.

Results

BHB antagonised cardiac microvascular hyperpermeability and promoted claudin-5 generation in diabetic rats First we measured the effects of BHB on blood glucose and body weight in diabetic rats. Compared with the Con group, blood glucose was significantly higher throughout the experiment in the DM group, which was not reduced by BHB treatment (Fig. 1a). A decrease in body weight was observed in the DM group at 10 weeks vs Con, which was not reversed by BHB treatment (Fig. 1b). Typical cardiac microvascular endothelial changes were evaluated by H&E staining (Fig. 1c). Intact endothelium was observed in the Con group, while the endothelium was deteriorating with disordered arrangement of myocardial fibres in the DM group. However, the

endothelium exhibited partial deterioration with regularly arranged myocardial fibres in the BHB2 and BHB3 groups.

FITC-dextran was used to measure cardiac microvascular permeability (Fig. 1d). Although not observed in the Con group, FITC fluorescence was distinctive in the DM group, reflecting microvascular hyperpermeability. The fluorescence was dramatically diminished in the BHB groups, particularly the BHB2 group. In addition, FITC fluorescence in mesenteric microvessels provided consistent directly feasible results of microvascular permeability, which showed bright FITC fluorescence in the DM group and obviously weakening of the signal in the BHB groups, especially the BHB2 group (ESM Fig. 1).

These results indicated that BHB could antagonise cardiac microvascular endothelial injury and hyperpermeability in the diabetic rats, without affecting blood glucose.

Next, we evaluated mRNA expression and protein content of claudin-5 (Fig. 2a, b). Compared with the Con group, claudin-5 mRNA expression and protein content were considerably decreased in the DM group, but were significantly

Fig. 2 BHB elevated claudin-5 generation in the cardiac microvasculature in diabetic rats. (**a, b**) *Claudin-5* mRNA expression (**a**; $n = 6$) and claudin-5 protein content (**b**; $n = 3$) in rats treated with STZ alone (DM), or STZ plus different concentrations of BHB (160 mg kg^{-1} day^{-1} BHB [BHB1], 200 mg kg^{-1} day^{-1} BHB [BHB2] or 240 mg kg^{-1} day^{-1} BHB [BHB3]) for 10 weeks. Data are means±SD. (**c**) Immunofluorescence of claudin-5 (red) and the endothelial marker CD31 (green) showing the typical microvascular claudin-5 distribution following BHB2 treatment. Scale bars, 20 μm. Images are representative of ten visual fields per group. *$p < 0.05$ vs Con; †$p < 0.05$ vs DM; analysed by one-way ANOVA and least significant difference test
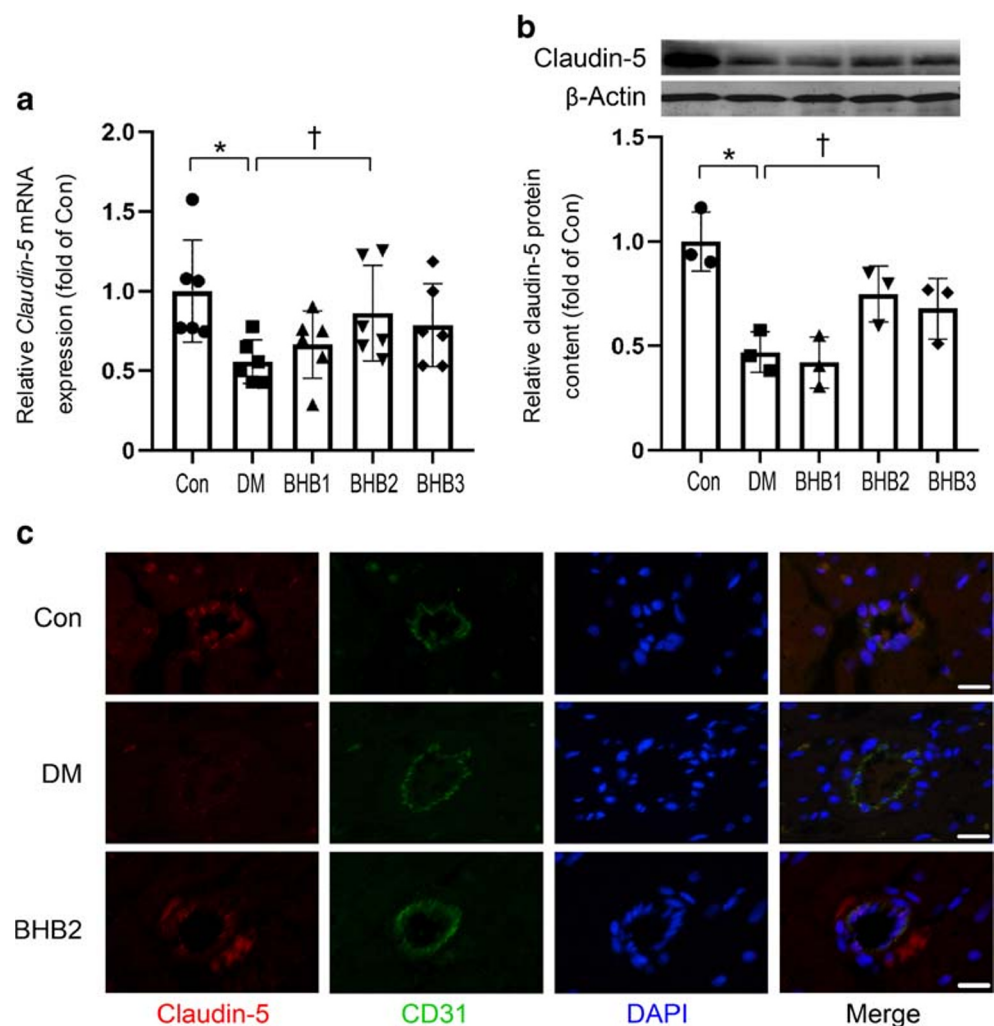
elevated in the BHB2 group vs DM. Therefore, cardiac microvascular distribution of claudin-5 was illustrated for BHB2 treatment (Fig. 2c). Immunofluorescence of claudin-5 in the cardiac microvasculature was obviously weakened in the DM group, and was conspicuously reversed in the BHB2 group, consistent with the changes in claudin-5 expression. These results demonstrated that BHB could antagonise cardiac microvascular hyperpermeability and promote claudin-5 generation in diabetic rats.

BHB promoted claudin-5 generation and attenuated paracellular hyperpermeability in HG-stimulated HCMECs

The mRNA expression of *Claudin-5* and paracellular permeability were measured to confirm the optimal concentration of HG stimulation for HCMECs (ESM Fig. 2). Compared with the normal glucose (5 mmol/l) group, *Claudin-5* mRNA expression decreased and paracellular permeability increased significantly with HG stimulation at 25 mmol/l, 30 mmol/l and 35 mmol/l. The results showed that 25 mmol/l HG was sufficient to suppress *Claudin-5* expression and cause paracellular hyperpermeability of HCMECs.

The effects of BHB on claudin-5 generation were examined in HG-stimulated HCMECs. Compared with the LG group, claudin-5 mRNA expression and protein content decreased notably in the HG group, but the decrease was non-significant in the L-HG group (Fig. 3a, b). However, the HG-induced suppression of claudin-5 was reversed with BHB treatment in a concentration-dependent manner, with a
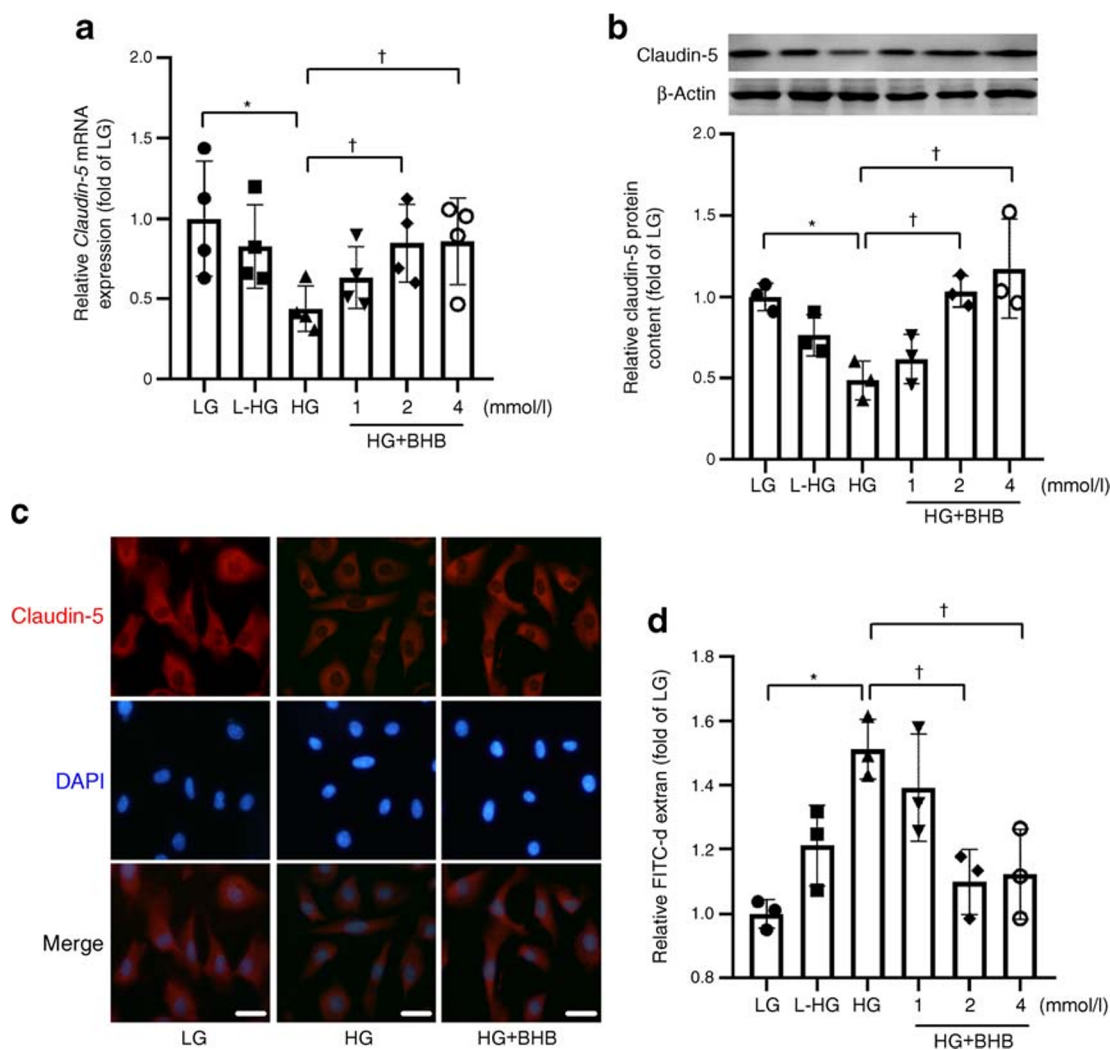

Fig. 3 BHB promoted claudin-5 generation and attenuated paracellular hyperpermeability in HG-stimulated HCMECs. (**a**, **b**) *Claudin-5* mRNA expression (**a**; $n = 4$) and claudin-5 protein content (**b**; $n = 3$) in HCMECs treated with HG or different concentrations of BHB. (**c**) Immunofluorescence showing the typical cellular distribution and content of claudin-5 (red) following LG treatment or HG treatment with or without 2 mmol/l BHB. Scale bars, 20 μm. Images are representative of ten visual fields per group. (**d**) FITC-dextran was used to measure paracellular (endothelial) permeability in HCMECs ($n = 3$). Data are means±SD. $*p < 0.05$ vs LG; $^†p < 0.05$ vs HG group; analysed by one-way ANOVA and least significant difference test

significant increase in the 2 mmol/l and 4 mmol/l BHB groups vs HG. Additionally, the immunofluorescence distribution of cellular claudin-5 was distinctly weakened under HG stimulation, but noticeably re-appeared with 2 mmol/l BHB treatment (Fig. 3c).

FITC-dextran was used to measure the paracellular permeability of HCMECs. Compared with the LG group, paracellular permeability increased conspicuously in the HG group. However, this was significantly reduced with the addition of 2 mmol/l and 4 mmol/l BHB to HG treatment, as compared with the HG group (Fig. 3d). These data manifested that BHB could promote claudin-5 generation and attenuate paracellular hyperpermeability in HG-stimulated HCMECs in a concentration-dependent manner.

BHB prevented HDAC3 from binding to the *Claudin-5* promoter in HG-stimulated HCMECs The contents and nuclear translocation of β-catenin, the transcriptional regulator of *Claudin-5* expression, were examined. Treatment with HG with or without BHB did not lead to significant changes in either the total or nuclear content of β-catenin in HCMECs (Fig. 4a, b). The results were corroborated by immunofluorescence of β-catenin under treatment with HG with or without 2 mmol/l BHB (Fig. 4c). The predicted β-catenin binding site in the *Claudin-5* promoter is illustrated in Fig. 5a. We performed a DNA pull-down assay to analyse the content of β-catenin bound to the *Claudin-5* promoter (Fig. 5b). No significant differences were found among the treatment groups for the calculated ratio of pull-down β-catenin to its input. The ChIP assay results confirmed that the level of

Claudin-5 promoter bound by β-catenin was similar between the treatment groups (Fig. 5c).

We also examined the content of *Claudin-5* promoter-bound HDAC1, HDAC3 and p300 by DNA pull-down assay (Fig. 5d), and the ratios of pull-down HDAC1, HDAC3 and p300 to their inputs were calculated to show relative promoter-bound protein content (Fig. 5e). Compared with the LG group, bound HDAC3 was decreased in the BHB group but increased in the HG group. Furthermore, BHB treatment significantly reduced the HG-induced increase in bound HDAC3, but had no significant effect on bound HDAC1 or p300. These results showed that BHB prevented HDAC3 from binding to the *Claudin-5* promoter in HG-stimulated HCMECs, without affecting β-catenin indicators.

BHB inhibited the interaction between HDAC3 and β-catenin in HG-stimulated HCMECs Next we evaluated the binding of HDAC1, HDAC3 and p300 to β-catenin using Co-IP. For β-catenin immunoprecipitation, the contents of co-immunoprecipitated HDAC1, HDAC3 and p300 were detected (Fig. 6a). The ratios of co-immunoprecipitated HDAC1, HDAC3 and p300 to their respective input values were calculated to show the relative bound content (Fig. 6b). Compared with the LG group, only HDAC3 content increased significantly in the HG group, but this increase was significantly reduced by BHB treatment. In parallel, for HDAC3 immunoprecipitation, the content of co-immunoprecipitated β-catenin was detected and calculated (Fig. 6c, d). Compared with the LG group, β-catenin content increased noticeably in the HG group, but was significantly decreased in the HG+BHB group.
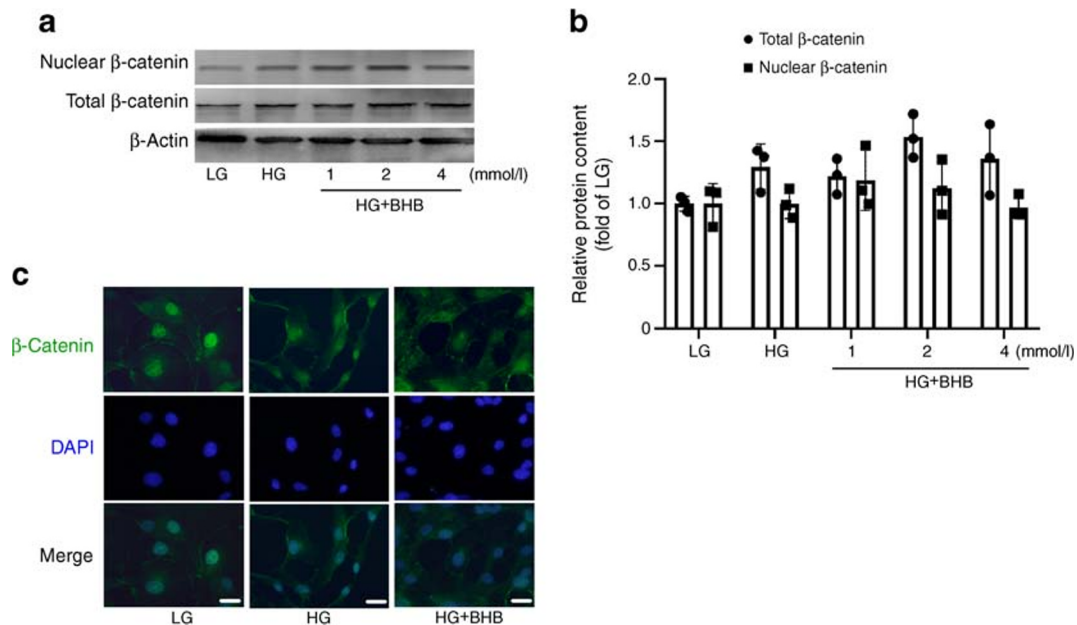

Fig. 4 BHB had little effect on the nuclear translocation of β-catenin. (**a**, **b**) The nuclear and total content of β-catenin was measured (**a**) and the ratio of nuclear:total β-catenin was calculated to reflect its nuclear translocation (**b**; $n = 3$). Data are means±SD; analysed by one-way ANOVA and least significant difference test. (**c**) Cellular distribution and content of β-catenin (green) following LG treatment or HG treatment with or without 2 mmol/l BHB. Scale bars, 20 μm
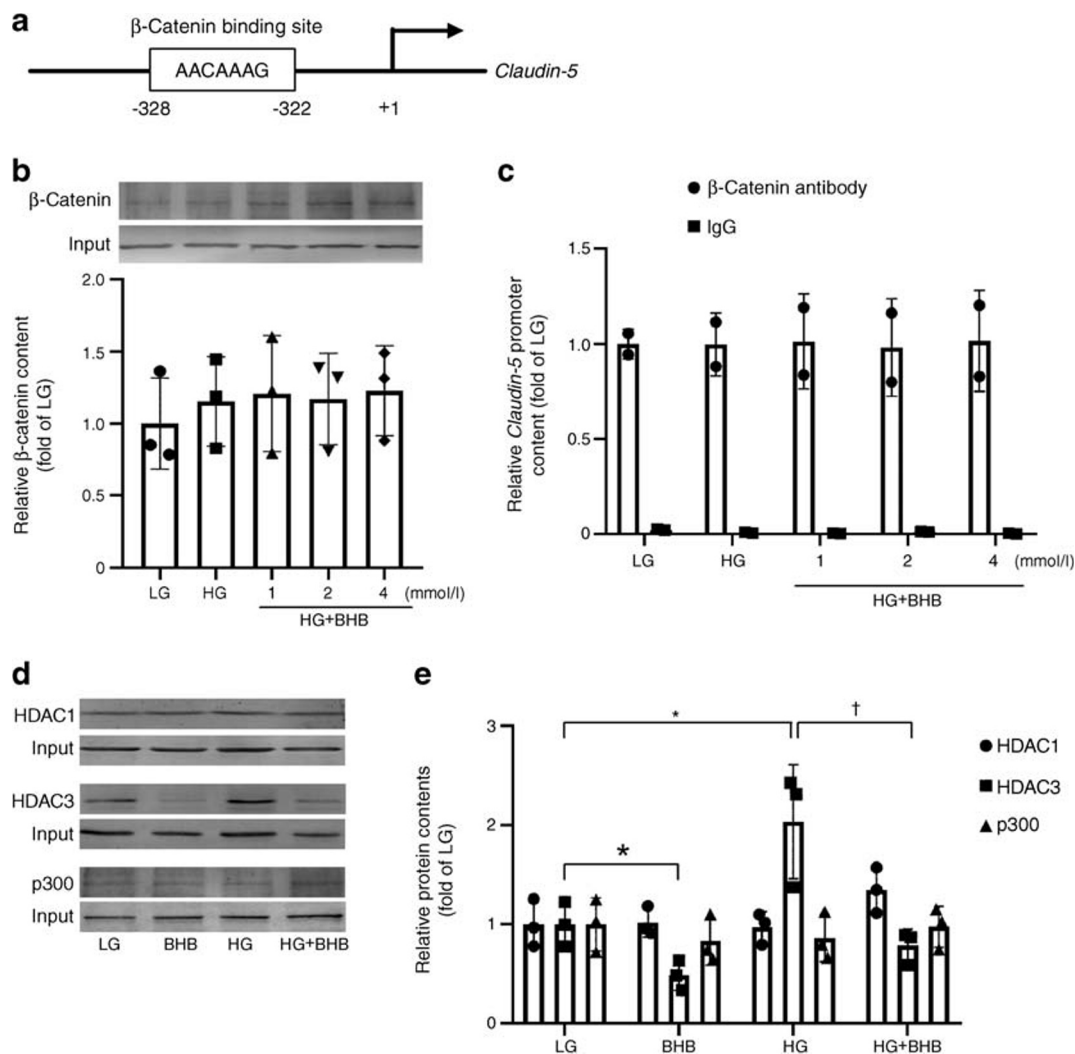
Fig. 5 BHB prevented HDAC3 from binding to the *Claudin-5* promoter. (a) Predicted β-catenin binding site in the *Claudin-5* promoter. (b) The relative content of β-catenin bound to its site in the *Claudin-5* promoter was measured by DNA pull-down assay and quantified ($n = 3$). (c) Relative content of *Claudin-5* promoter bound by β-catenin, as detected by ChIP ($n = 2$). (d) Binding of HDAC1, HDAC3 and p300 to the β-catenin binding site in the *Claudin-5* promoter, as measured by DNA pull-down assay. (e) Calculated ratios of bound HDAC1, HDAC3 and p300 to their total content ('input') to show relative bound content ($n = 3$). Data are means±SD. *$p < 0.05$ vs LG; †$p < 0.05$ vs HG; analysed by one-way ANOVA and least significant difference test

The co-localisation of HDAC3 and β-catenin was also observed by confocal scanning microscopy (Fig. 7). Although no obvious differences were found among the groups in the contents of HDAC3 and β-catenin, there was a distinctive co-localisation of HDAC3 and β-catenin in the HG group. However, the HG-stimulated co-localisation of HDAC3 and β-catenin was overtly inhibited by BHB treatment. These results suggested that BHB inhibited the binding and co-localisation of HDAC3 and β-catenin in HG-stimulated HCMECs.

BHB caused specific increases in H3K14ac in the *Claudin-5* promoter Since BHB inhibited the binding of HDAC3 to both the *Claudin-5* promoter and β-catenin, we measured histone acetylation in the promoter-binding site for β-catenin. After

DNA pull-down with the *Claudin-5* promoter sequence containing the β-catenin binding site, histone acetylations were analysed using mass spectrometry (Fig. 8a). The results identified specific H3K14ac modification in both the BHB and HG+BHB groups.

First, we examined the total content of the identified H3K14ac, as well as general H3K9ac modifications (ESM Fig. 3). Neither H3K14ac nor H3K9ac showed significant differences between the groups. Following this, the contents of H3K14ac and H3K9ac in the *Claudin-5* promoter were measured by DNA pull-down assay (Fig. 8b). The ratios of pull-down H3K9ac or H3K14ac to H3 were calculated to show the relative content of each (Fig. 8c). Although no significant difference was observed between the LG and HG groups for H3K14ac, its content increased significantly in the BHB and HG+BHB groups vs
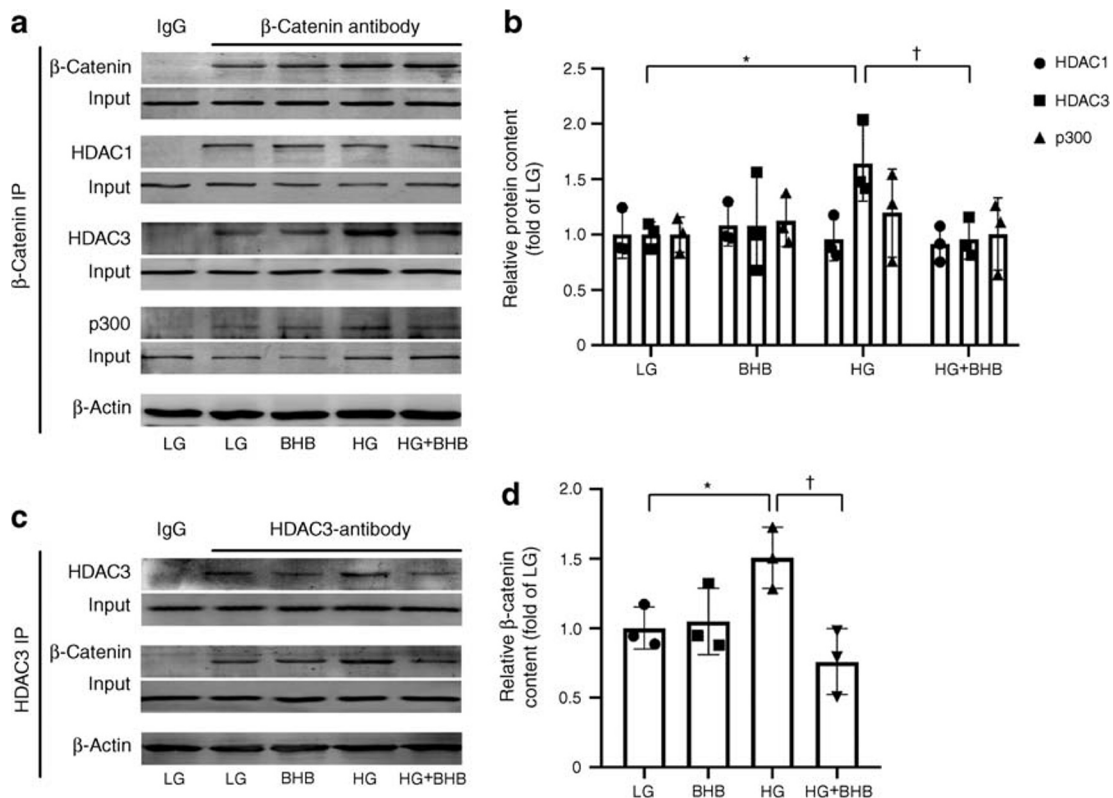
Fig. 6 BHB inhibited the binding of HDAC3 to β-catenin. (a) Measurement of HDAC1, HDAC3 and p300 content after β-catenin immunoprecipitation (IP). (b) Calculated ratios of immunoprecipitated HDAC1, HDAC3 and p300 to their total content ('input') (n = 3). (c) Measurement of β-catenin after HDAC3 IP. (d) Calculated ratio of immunoprecipitated β-catenin to total content ('input') (n = 3). Data are means±SD. *p < 0.05 vs LG; †p < 0.05 vs HG; analysed by one-way ANOVA and least significant difference test

LG and HG, respectively. In contrast, compared with that in the LG group, H3K9ac content decreased in the HG group, but was not significantly affected by BHB treatment.

These results confirmed that BHB treatment caused specific increases in H3K14ac in the *Claudin-5* promoter, activating claudin-5 transcription.
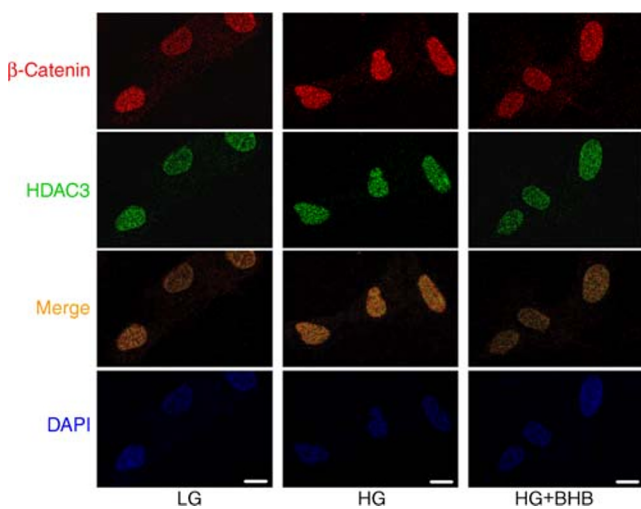

Fig. 7 BHB inhibited the co-localisation of β-catenin and HDAC3. Confocal scanning microscopy showing the co-localisation (yellow) of β-catenin (red) and HDAC3 (green) following LG treatment or HG treatment with or without 2 mmol/l BHB. Scale bars, 10 μm

Discussion

In this study, we found that BHB promoted claudin-5 generation and antagonised cardiac microvascular hyperpermeability in the STZ-induced diabetes rat model. In addition, under HG stimulation, BHB was found to promote claudin-5 generation and attenuated paracellular hyperpermeability in HCMECs in a concentration-dependent manner. Our data also clarified that HG stimulation provoked HDAC3 and reduced H3K9ac in the *Claudin-5* promoter to suppress claudin-5 expression. In contrast, BHB treatment inhibited HDAC3 and caused a specific increase in H3K14ac in the *Claudin-5* promoter, thereby activating claudin-5 generation.

Endothelial dysfunction is the initial pathological factor in cardiac microvascular diseases, and disruption of tight junctions, a hallmark event of endothelial barrier dysfunction, leads to cardiac microvascular hyperpermeability in individuals with diabetes [29, 30]. Clinical studies have suggested that individuals with microvascular complications are at
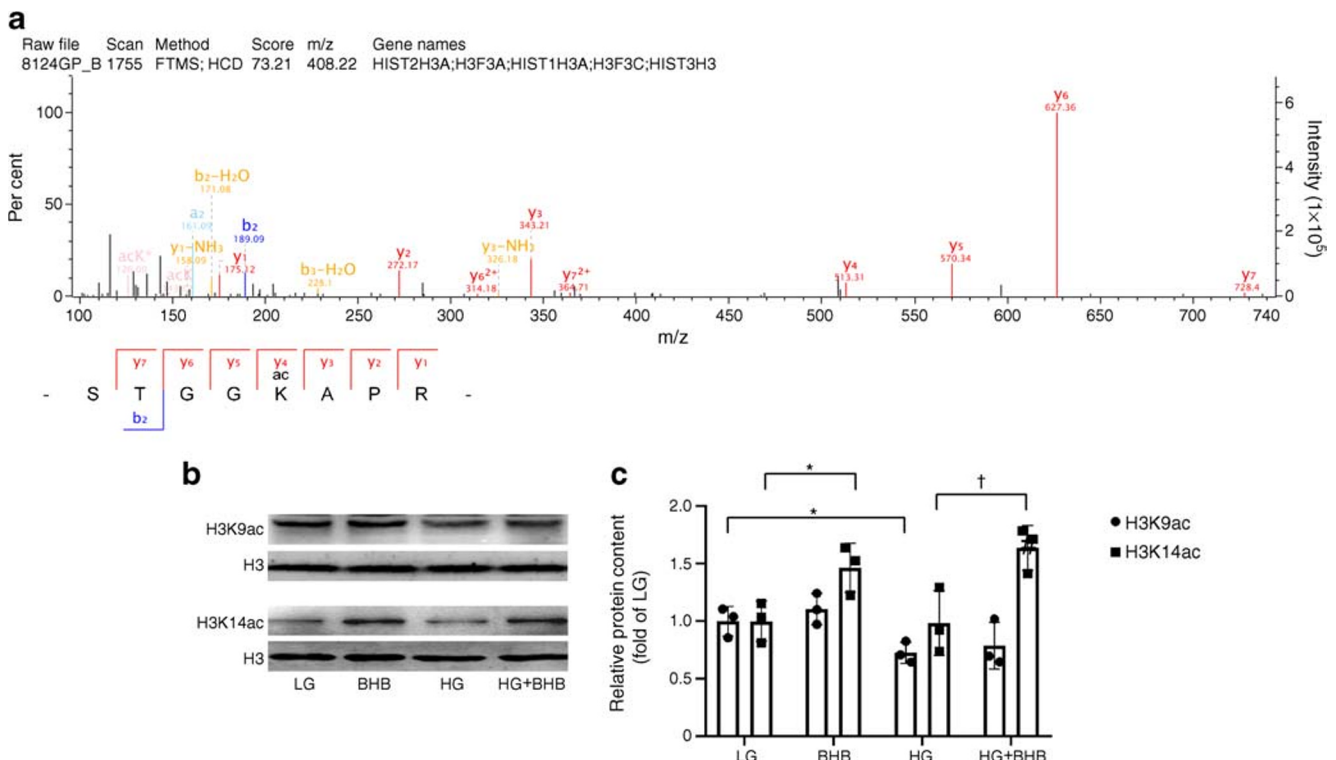
Fig. 8 BHB caused specific H3K14ac modification in the *Claudin-5* promoter. (**a**) Following DNA pull-down assay with the *Claudin-5* promoter sequence containing β-catenin binding site, mass spectrometry analysis of histone acetylation identified specific presence of H3K14ac with BHB treatment ($n = 2$). (**b**) Verification of the presence of H3K9ac and H3K14ac in the *Claudin-5* promoter. (**c**) Calculated ratios of bound H3K9ac and H3K14ac to H3 to show their relative content ($n = 3$). Data are means±SD. *$p < 0.05$ vs LG; †$p < 0.05$ vs HG; analysed by one-way ANOVA and least significant difference test

increased risk of dilated cardiomyopathy, indicating the importance of endothelial hyperpermeability in the pathogenesis of cardiomyopathy [31]. We also observed both mesenteric and cardiac microvascular hyperpermeability, with disorderly arrangement of myocardial fibres being observed in the diabetic rats. Several studies have emphasised the importance of claudin-5 in brain microvascular hyperpermeability, including in diabetic conditions [8, 32]. In addition, in individuals with diabetic macular oedema, inflammation-induced claudin-5 redistribution leads to blood–retinal barrier disruption [9]. Our results confirmed the presence of claudin-5 insufficiency and endothelial hyperpermeability in the cardiac microvasculature under diabetic conditions. However, indicators for β-catenin, the transcriptional regulator of claudin-5, showed minimal changes under HG stimulation in this study.

The acetyltransferase p300 and HDACs are positive and negative controllers of histone acetylation, respectively, comprising an on/off switch for gene transactivation [13–15]. p300 may participate in the transactivation of pathological genes in diabetes, and p300 inhibitors have been reported to reverse hypertension-induced cardiac hypertrophy and fibrosis [13, 27]. HDACs play pathogenic and protective roles depending on the disease, and HDAC3 inhibition may have therapeutic potential for cardiovascular diseases [33]. Our results showed that HDAC3 binding to both the

Claudin-5 promoter and β-catenin increased significantly under HG stimulation. Additionally, the critical histone activation marker H3K9ac, which is a deacetylation target of HDAC3 [34], was found to be decreased in the *Claudin-5* promoter under HG stimulation, consistent with our previous study [10]. Therefore, HG conditions may provoke HDAC3 to reduce the amount of H3K9ac bound to the *Claudin-5* promoter, suppressing its transcription. However, an effective therapy for claudin-5 insufficiency and cardiac microvascular hyperpermeability in individuals with diabetes is lacking.

Recently, BHB was found to have unique protective effects on the cardiovascular system [35, 36]. The injured heart relies more heavily on ketone bodies as an energy source [19, 37]. BHB, which can be produced via the practice of intermittent fasting or administered directly, is believed to improve cardiovascular function and extend healthspan [16, 38–40]. Besides being an energy source, BHB prevents endothelial cell senescence [20, 21]. Even in diabetes, the administration of BHB is reported to alleviate retinopathy and nephropathy [41, 42]. Based on our serial investigations [22, 23], this study found that BHB could promote claudin-5 generation and antagonise diabetes-associated cardiac microvascular hyperpermeability in vivo and in vitro. Clinical studies have proved that oral administration of BHB has beneficial effects for participants, indicating its potential clinical application
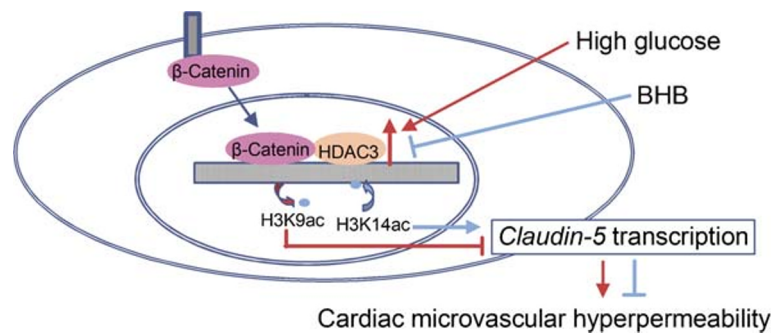
Fig. 9 BHB inhibited HDAC3 and caused specific increases in H3K14ac to activate claudin-5 generation and attenuate diabetes-associated cardiac endothelial hyperpermeability. Under HG stimulation, β-catenin recruited HDAC3 to the *Claudin-5* promoter to reduce H3K9ac levels, thereby suppressing claudin-5 expression and causing cardiac microvascular hyperpermeability. BHB treatment inhibited HDAC3 and caused specific increases in H3K14ac in the *Claudin-5* promoter, which promoted claudin-5 generation and attenuated diabetic cardiac endothelial hyperpermeability

[43–45]. Usually, a 2 mmol/l threshold concentration of BHB is required for its effective treatment [17], which was also confirmed by our data. The results from this study may provide important evidence for extended applications of BHB. Although BHB is reportedly helpful for glucose control in individuals with obesity [45], our data showed no effect of BHB on blood glucose in diabetic rats, which may be attributed to our use of the STZ-induced type 1 diabetes model. Therefore, the potential effects of BHB on blood glucose should be further investigated in type 2 diabetes models.

Several mechanisms have been proposed for the protective effects of BHB [18, 20, 24, 25]. It is reported that BHB could modulate functions of transcriptional factors to exert anti-inflammatory actions [46]. In this study, however, BHB did not exhibit any effect on β-catenin indicators. Notably, BHB has been reported to be an inhibitor of HDACs, to activate gene transcription and play protective roles [47, 48]. We found that BHB inhibited HG-induced HDAC3 from binding to the *Claudin-5* promoter and β-catenin. HDAC3 inhibition has been shown to prevent blood–brain barrier permeability through activation of nuclear factor erythroid 2–related factor 2 (Nrf2) in male type 2 diabetes mouse models [49]. Our results manifested that BHB inhibited the activity of the key controller, HDAC3, to promote claudin-5 generation in HG-stimulated HCMECs.

Using mass spectrometry analysis of histone acetylation, we identified specific presence of H3K14ac in the *Claudin-5* promoter under treatment with BHB. The changes in H3K9ac and H3K14ac, which are the most significant sites for acetylation, vary under different conditions [50]. In this study, HG provoked HDAC3 and reduced H3K9ac in the *Claudin-5* promoter, suppressing claudin-5 expression. However, BHB markedly inhibited HDAC3, causing a specific increase in H3K14ac in the *Claudin-5* promoter, regardless of the presence of HG. These results hinted at a general mechanism of BHB

inhibition of HDAC3 to promote claudin-5-mediated attenuation of endothelial hyperpermeability, contributing to our understanding of the cardiovascular protective effects of BHB. However, the underlying mechanism for the regulation of H3K9ac and H3K14ac requires further clarification.

In conclusion, these data demonstrated that HG stimulation provoked the binding of HDAC3 to the *Claudin-5* promoter and β-catenin to reduce H3K9ac levels, suppressing *Claudin-5* transcription and triggering cardiac microvascular hyperpermeability; BHB treatment inhibited HDAC3 and caused a specific increase in H3K14ac levels in the *Claudin-5* promoter, to 'turn on' claudin-5 generation and attenuate diabetic cardiac microvascular hyperpermeability (Fig. 9). These data may provide important evidence for the cardiovascular protective effects of BHB, facilitating its clinical application.

Authors' relationships and activities The authors declare that there are no relationships or activities that might bias, or be perceived to bias, their work.

Contribution statement YL and JQ conceived and designed the project. BL, YY and KL conducted the cell experiments and analysed data. YZ, QG and FZ performed animal experiments. BL, YY, KL and YL interpreted the results. YL and JQ wrote the manuscript. BL, YY and KL contributed equally to this work. All authors contributed to editing the article and approved the final version to be published. YL and JQ are the guarantors of this work.

References

1. Dal Canto E, Ceriello A, Rydén L et al (2019) Diabetes as a cardiovascular risk factor: an overview of global trends of macro and micro vascular complications. Eur J Prev Cardiol 26(2_suppl):25–32. https://doi.org/10.1177/2047487319878371

2. Liu YL, Zhou XY, Xuan LJ (2019) Magnesium lithospermate B ameliorates microcirculation perfusion in rats by promoting vascular NO production via activating the PI3K/AKT pathway. Acta Pharmacol Sin 40(8):1010–1018. https://doi.org/10.1038/s41401-018-0203-7

3. Inzucchi SE, Viscoli CM, Young L et al (2019) Diabetes prevention and cardiovascular complications. Diabetologia 62(11):2161–2162. https://doi.org/10.1007/s00125-019-04999-3

4. Garcia-Vaz E, McNeilly AD, Berglund LM et al (2020) Inhibition of NFAT signaling restores microvascular endothelial function in diabetic mice. Diabetes 69(3):424–435. https://doi.org/10.2337/db18-0870

5. Cong X, Kong W (2020) Endothelial tight junctions and their regulatory signaling pathways in vascular homeostasis and disease. Cell Signal 66:109485. https://doi.org/10.1016/j.cellsig.2019.109485

6. Li XX, Ling SK, Hu MY, Ma Y, Li Y, Huang PL (2019) Protective effects of acarbose against vascular endothelial dysfunction through inhibiting Nox4/NLRP3 inflammasome pathway in diabetic rats. Free Radic Biol Med 145:175–186. https://doi.org/10.1016/j.freeradbiomed.2019.09.015

7. Juni RP, Kuster DWD, Goebel M et al (2019) Cardiac microvascular endothelial enhancement of cardiomyocyte function is impaired by inflammation and restored by empagliflozin. JACC Basic Transl Sci 4(5):575–591. https://doi.org/10.1016/j.jacbts.2019.04.003

8. Greene C, Hanley N, Campbell M (2019) Claudin-5: gatekeeper of neurological function. Fluids Barriers CNS 16(1):3. https://doi.org/10.1186/s12987-019-0123-z

9. Arima M, Nakao S, Yamaguchi M et al (2020) Claudin-5 redistribution induced by inflammation leads to anti-VEGF-resistant diabetic macular edema. Diabetes 69(5):981–999. https://doi.org/10.2337/db19-1121

10. Li B, Li Y, Liu K et al (2017) High glucose decreases claudins-5 and -11 in cardiac microvascular endothelial cells: antagonistic effects of tongxinluo. Endocr Res 42(1):15–21. https://doi.org/10.3109/07435800.2016.1163723

11. Tran KA, Zhang X, Predescu D et al (2016) Endothelial β-catenin signaling is required for maintaining adult blood-brain barrier integrity and central nervous system homeostasis. Circulation 133(2):177–186. https://doi.org/10.1161/CIRCULATIONAHA.115.015982

12. Morini MF, Giampietro C, Corada M et al (2018) VE-cadherin-mediated epigenetic regulation of endothelial gene expression. Circ Res 122(2):231–245. https://doi.org/10.1161/CIRCRESAHA.117.312392

13. Rai R, Sun T, Ramirez V et al (2019) Acetyltransferase p300 inhibitor reverses hypertension-induced cardiac fibrosis. J Cell Mol Med 23(4):3026–3031. https://doi.org/10.1111/jcmm.14162

14. Zhao TC, Wang Z, Zhao TY (2020) The important role of histone deacetylases in modulating vascular physiology and arteriosclerosis. Atherosclerosis 303:36–42. https://doi.org/10.1016/j.atherosclerosis.2020.04.020

15. Emmett MJ, Lazar MA (2019) Integrative regulation of physiology by histone deacetylase 3. Nat Rev Mol Cell Biol 20(2):102–115. https://doi.org/10.1038/s41580-018-0076-0

16. Stekovic S, Hofer SJ, Tripolt N et al (2019) Alternate day fasting improves physiological and molecular markers of aging in healthy, non-obese humans. Cell Metab 30(3):462–476. https://doi.org/10.1016/j.cmet.2019.07.016

17. Margolis LM, O'Fallon KS (2020) Utility of ketone supplementation to enhance physical performance: a systematic review. Adv Nutr 11(2):412–419. https://doi.org/10.1093/advances/nmz104

18. Newman JC, Verdin E (2017) β-Hydroxybutyrate: a signaling metabolite. Annu Rev Nutr 37(1):51–76. https://doi.org/10.1146/annurev-nutr-071816-064916

19. Mizuno Y, Harada E, Nakagawa H et al (2017) The diabetic heart utilizes ketone bodies as an energy source. Metabolism 77:65–72. https://doi.org/10.1016/j.metabol.2017.08.005

20. Han YM, Bedarida T, Ding Y et al (2018) β-Hydroxybutyrate prevents vascular senescence through hnRNP A1-mediated upregulation of Oct4. Mol Cell 71(6):1064–1078. https://doi.org/10.1016/j.molcel.2018.07.036

21. Arildsen L, Andersen JV, Waagepetersen HS, Nissen JBD, Sheykhzade M (2019) Hypermetabolism and impaired endothelium-dependent vasodilation in mesenteric arteries of type 2 diabetes mellitus db/db mice. Diab Vasc Dis Res 16(6):539–548. https://doi.org/10.1177/1479164119865885

22. Wu X, Miao D, Liu Z et al (2020) β-Hydroxybutyrate antagonizes aortic endothelial injury by promoting generation of VEGF in diabetic rats. Tissue Cell 64:101345. https://doi.org/10.1016/j.tice.2020.101345

23. Luo W, Yu Y, Wang H et al (2020) Up-regulation of MMP-2 by histone H3K9 β-hydroxybutyrylation to antagonize glomerulosclerosis in diabetic rat. Acta Diabetol https://doi.org/10.1007/s00592-020-01552-2

24. Miyamoto J, Ohue-Kitano R, Mukouyama H et al (2019) Ketone body receptor GPR43 regulates lipid metabolism under ketogenic conditions. Proc Natl Acad Sci U S A 116(47):23813–23821. https://doi.org/10.1073/pnas.1912573116

25. Neudorf H, Durrer C, Myette-Cote E, Makins C, O'Malley T, Little JP (2019) Oral ketone supplementation acutely increases markers of NLRP3 inflammasome activation in human monocytes. Mol Nutr Food Res 63(11):e1801171. https://doi.org/10.1002/mnfr.201801171

26. Rojas-Morales P, Pedraza-Chaverri J, Tapia E (2020) Ketone bodies, stress response, and redox homeostasis. Redox Biol 29:101395. https://doi.org/10.1016/j.redox.2019.101395

27. Li Y, Li X, He K et al (2018) C-peptide prevents NF-κB from recruiting p300 and binding to the *inos* promoter in diabetic nephropathy. FASEB J 32(4):2269–2279. https://doi.org/10.1096/fj.201700891R

28. Natarajan R, Northrop N, Yamamoto B (2017) Fluorescein isothiocyanate (FITC)-dextran extravasation as a measure of blood-brain barrier permeability. Curr Protoc Neurosci 79:9.58.1–9.58.15. https://doi.org/10.1002/cpns.25

29. Gamrat A, Surdacki MA, Chyrchel B, Surdacki A (2020) Endothelial dysfunction: a contributor to adverse cardiovascular remodeling and heart failure development in type 2 diabetes beyond accelerated atherogenesis. J Clin Med 9(7):E2090. https://doi.org/10.3390/jcm9072090

30. Mordi IR, Tee A, Palmer CN, McCrimmon RJ, Doney ASF, Lang CC (2020) Microvascular disease and heart failure with reduced and preserved ejection fraction in type 2 diabetes. ESC Heart Fail 7(3):1168–1177. https://doi.org/10.1002/ehf2.12669

31. Cheung N, Wang JJ, Rogers SL et al (2008) Diabetic retinopathy and risk of heart failure. J Am Coll Cardiol 51(16):1573–1578. https://doi.org/10.1016/j.jacc.2007.11.076

32. Rom S, Heldt NA, Gajghate S, Seliga A, Reichenbach NL, Persidsky Y (2020) Hyperglycemia and advanced glycation end products disrupt BBB and promote occludin and claudin-5 protein secretion on extracellular microvesicles. Sci Rep 10(1):7274. https://doi.org/10.1038/s41598-020-64349-x

33. Zhang L, Chen Y, Jiang Q, Song W, Zhang L (2019) Therapeutic potential of selective histone deacetylase 3 inhibition. Eur J Med Chem 162:534–542. https://doi.org/10.1016/j.ejmech.2018.10.072

34. Ji H, Zhou Y, Zhuang X et al (2019) HDAC3 deficiency promotes liver cancer through a defect in H3K9ac/H3K9me3 transition. Cancer Res 79(14):3676–3688. https://doi.org/10.1158/0008-5472.CAN-18-3767

35. Abdul Kadir A, Clarke K, Evans RD (2020) Cardiac ketone body metabolism. Biochim Biophys Acta Mol basis Dis 1866(6):165739. https://doi.org/10.1016/j.bbadis.2020.165739

36. Place DE, Kanneganti TD (2019) Fueling ketone metabolism quenches salt-induced hypertension. Trends Endocrinol Metab 30(3):145–147. https://doi.org/10.1016/j.tem.2019.01.004

37. Horton JL, Davidson MT, Kurishima C et al (2019) The failing heart utilizes 3-hydroxybutyrate as a metabolic stress defense. JCI Insight 4(4):e124079. https://doi.org/10.1172/jci.insight.124079

38. Han YM, Ramprasath T, Zou MH (2020) β-Hydroxybutyrate and its metabolic effects on age-associated pathology. Exp Mol Med 52(4):548–555. https://doi.org/10.1038/s12276-020-0415-z

39. Nielsen R, Møller N, Gormsen LC et al (2019) Cardiovascular effects of treatment with the ketone body 3-hydroxybutyrate in chronic heart failure patients. Circulation 139(18):2129–2141. https://doi.org/10.1161/CIRCULATIONAHA.118.036459

40. Soto-Mota A, Norwitz NG, Clarke K (2020) Why a D-β-hydroxybutyrate monoester? Biochem Soc Trans 48(1):51–59. https://doi.org/10.1042/BST20190240

41. Trotta MC, Maisto R, Guida F et al (2019) The activation of retinal HCA2 receptors by systemic beta-hydroxybutyrate inhibits diabetic retinal damage through reduction of endoplasmic reticulum stress and the NLRP3 inflammasome. PLoS One 14(1):e0211005. https://doi.org/10.1371/journal.pone.0211005

42. Kimura Y, Kuno A, Tanno M et al (2019) Canagliflozin, a sodium-glucose cotransporter 2 inhibitor, normalizes renal susceptibility to type 1 cardiorenal syndrome through reduction of renal oxidative stress in diabetic rats. J Diabetes Investig 10(4):933–946. https://doi.org/10.1111/jdi.13009

43. Stubbs BJ, Cox PJ, Evans RD et al (2017) On the metabolism of exogenous ketones in humans. Front Physiol 8:848. https://doi.org/10.3389/fphys.2017.00848

44. Soto-Mota A, Vansant H, Evans RD, Clarke K (2019) Safety and tolerability of sustained exogenous ketosis using ketone monoester drinks for 28 days in healthy adults. Regul Toxicol Pharmacol 109:104506. https://doi.org/10.1016/j.yrtph.2019.104506

45. Myette-Côté É, Caldwell HG, Ainslie PN, Clarke K, Little JP (2019) A ketone monoester drink reduces the glycemic response to an oral glucose challenge in individuals with obesity: a randomized trial. Am J Clin Nutr 110(6):1491–1501. https://doi.org/10.1093/ajcn/nqz232

46. Kim DH, Park MH, Ha S et al (2019) Anti-inflammatory action of β-hydroxybutyrate via modulation of PGC-1α and FoxO1, mimicking calorie restriction. Aging 11(4):1283–1304. https://doi.org/10.18632/aging.101838

47. Cheng CW, Biton M, Haber AL et al (2019) Ketone body signaling mediates intestinal stem cell homeostasis and adaptation to diet. Cell 178(5):1115–1131. https://doi.org/10.1016/j.cell.2019.07.048

48. Li X, Zhan Z, Zhang J, Zhou F, An L (2020) β-Hydroxybutyrate ameliorates Aβ-induced downregulation of TrkA expression by inhibiting HDAC1/3 in SH-SY5Y cells. Am J Alzheimers Dis Other Dement 35:1533317519883496. https://doi.org/10.1177/1533317519883496

49. Zhao Q, Zhang F, Yu Z et al (2019) HDAC3 inhibition prevents blood-brain barrier permeability through Nrf2 activation in type 2 diabetes male mice. J Neuroinflammation 16(1):103. https://doi.org/10.1186/s12974-019-1495-3

50. Jarmasz JS, Stirton H, Davie JR, Del Bigio MR (2019) DNA methylation and histone post-translational modification stability in post-mortem brain tissue. Clin Epigenetics 11(1):5. https://doi.org/10.1186/s13148-018-0596-7